

Importance of transverse dipoles in the stability of biaxial nematic phase: A Monte Carlo study

Nababrata Ghoshal, Kisor Mukhopadhyay¹ and Soumen Kumar Roy^{2, *}

Department of Physics, Mahishadal Raj College,
Mahishadal, Purba-Medinipur, West Bengal, India

¹Department of Physics, Sundarban Mahavidyalaya,
Kakdwip, South 24 Parganas, West Bengal, India

²Department of Physics, Jadavpur University,
Kolkata - 700 032, India

Abstract

Monte Carlo simulation performed on a lattice system of biaxial molecules possessing D_{2h} symmetry and interacting with a second rank anisotropic dispersion potential yields three distinct macroscopic phases depending on the biaxiality of the constituent molecules. The phase diagram of such a system as a function of molecular biaxiality is greatly modified when a transverse dipole is considered to be associated with each molecule so that the symmetry is reduced to C_{2v} . Our results indicate the splitting of the Landau point i.e. the point in the phase diagram where a direct transition from the isotropic phase to the biaxial nematic phase occurs, into a Landau line for a system of biaxial molecules with strong transverse dipoles. The width of the Landau line becomes maximum for an optimal value of the relative dipolar strength. The presence of transverse dipoles leads to the stabilization of the thermotropic biaxial nematic phase

*Corresponding author. E-mail: skroy@phys.jdvu.ac.in, Tel: +91 9874741525; fax: +91 33 24146584

at higher temperature and for a range of values of molecular biaxiality. The structural properties in the uniaxial and biaxial phases are investigated by evaluating the first rank and second rank orientational correlation functions. The dipole induced long range order of the anti-ferroelectric structure in the biaxial nematic phase, is revealed.

1 Introduction

In the past few years great interest has been paid to thermotropic biaxial nematic liquid crystals, whose existence was first predicted by Freiser [1] in 1970 from mean field theory. Shortly afterwards, a number of theoretical [2, 3] and computer simulation [4, 5, 6] studies have been performed and phase diagrams consisting of three distinct macroscopic phases namely, the isotropic phase (I), the uniaxial nematic phase (N_U) (which may be, keeping the symmetry of the phase unchanged, of two types - prolate (N_{U+}) or oblate (N_{U-}) nematic phases depending on the rod-like or disk-like nature of the molecules) and biaxial nematic phase (N_B) were generated. On the experimental front, scientists have been engaged in search for truly biaxial nematic phase in thermotropic liquid crystals since its theoretical prediction. Although there have been a number of reports [7, 8] of experimental identification of thermotropic N_B phase since 1986, none of these claims proved to be correct [11]. Recently there have been claims of observing the elusive thermotropic N_B phase for V-shaped molecules [12, 13] and for tetrapode molecules [14, 15]. These new findings have fuelled experimental and theoretical research [16] on biaxiality in thermotropic liquid crystals.

The molecules forming liquid crystals always deviate from their assumed cylindrical symmetry and their usual structure can schematically be described as board-like (see Figure 1). Usually this type of molecules give rise to the N_U phase as a consequence of the long range orientational order of the molecular long symmetry axis (\mathbf{w}) while the short symmetry axes (\mathbf{u} , \mathbf{v}) remain uncorrelated except at short range. In this case the molecular long axes tend to be parallel, on average, along a single macroscopic direction called the principal director (\mathbf{n}). At some state point long range orientational ordering is established for the molecular long axes as well as for the molecular short axes which results in a biaxial nematic phase and the corresponding average preferential alignments of the short axes occur along

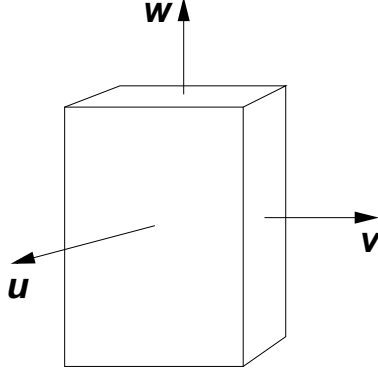


Figure 1: Schematic diagram of a biaxial molecule. Three molecular symmetry axes are \mathbf{u} , \mathbf{v} and \mathbf{w} .

the two secondary directors (\mathbf{l}, \mathbf{m}) .

The ability of a material to form the N_B phase depends on the molecular biaxiality of the constituent molecules. In the case of isotropically averaged dispersive interactions (which we have used in the present work) there is a single molecular biaxiality parameter λ [9, 10] which is related to the anisotropy of the polarizability tensor of the molecule. From the study of molecular field theory [11] it has been observed that for obtaining a stable N_B phase, λ must have values within a very narrow range around the optimal biaxiality (λ_C). The theoretical value of λ_C is $1/\sqrt{6}$ (≈ 0.40825), which corresponds to the transition point from a system of prolate to oblate molecules [5, 11, 17]. For this value a second-order transition occurs directly between biaxial and isotropic phases and the corresponding point in the phase diagram is known as the Landau point. At this special critical point where two second order critical lines meet a first order phase boundary, N_B phases are expected to appear at the highest temperature and therefore, on the basis of theoretical analysis one may predict that to be a good candidate towards forming the N_B phase the molecule should have the biaxiality very close to λ_C . But it is almost an impossible task for the experimentalists to design mesogenic molecules with the desired biaxiality due to molecular flexibility. However, influence of other factors, such as polydispersity [18], large transverse electric dipoles associated with the mesogenic molecules etc., enhances the stability of the N_B phase. The present scenario in context of the transverse dipole moments is elaborated below.

For symmetric bent-core molecules (V-shaped) the optimal biaxiality factor $\lambda_C = 1/\sqrt{6}$

occurs for a single angle of 109.47° between the arms which is the tetrahedral angle. On the other hand Madsen et. al. [12] while investigating a class of bent-core molecules with different angles between the arms claimed to have observed a biaxial phase at an inter-arm angle as large as 140° . At this angle the molecular biaxiality factor is such that a N_U phase is expected. Although the work of Madsen et. al. [12] does not give a conclusive evidence of the occurrence of a biaxial nematic, it may be noted that the type of molecules they considered had a strong transverse electric dipole moment. To find if this could in some way make the job of finding the biaxial nematic phase easier, Bates [19] performed a Monte Carlo simulation using a lattice model of bent-core molecules with transverse dipoles attached to the centre. In this work each molecule was assumed to have two symmetric arms and the included angle was varied. Each arm of a molecule interacts with each of the twelve arms of the six nearest neighbour molecules confined to a simple cubic lattice via the usual Lebwohl-Lasher potential [20]. In addition, the dipole-dipole interaction, which actually is of long range nature, was also confined to the nearest neighbours for simplicity and was taken to be of the $-\cos\beta$ type where β is the angle between the interacting dipoles. The phase diagram that Bates obtained was quite different from the usual one obtained while treating non-polar bend-core molecules where one gets a single Landau point for a bend angle of 109.47° . Instead, he observed that for large dipole moments the single Landau point gets transformed into a series of Landau points usually called a Landau line which covers a significant range of angles (and hence a range of molecular biaxiality) across which a direct $N_B \leftrightarrow I$ first order transition occurs. If this is really the case then the job of the experimentalists becomes a little easier.

On the theoretical front there is a very recent work on bent-core molecules by Grzybowski and Longa [21] who used density functional theory (DFT) to analyze two- and three-segment Gay-Berne (GB) molecules with a single transverse dipole moment. They found that nonpolar models with two uniaxial arms has a single Landau point and the inclusion of the dipoles shifts the Landau point towards lower apex angles for the system containing two-arm molecules. For the three-segment molecules with large dipole moments a Landau line occurs and they observe that for an optimal dipole strength the N_B phase is most probable. In all cases these authors show that further strengthening of the dipolar interaction results in shrinking the distance between the isotropic phase and the biaxial

nematic phase which indicates that the intermediate uniaxial nematic phase becomes less stable. The study reveals that in the most likely situation for detecting the N_B phase each molecule should consist of three segments with a transverse dipole moment of about $3D$.

In this communication we present the results of a Monte Carlo simulation in a lattice model where biaxial molecules of D_{2h} symmetry interact with nearest neighbours via an anisotropic dispersion potential. To study the effect of dipolar interaction on the phase behaviour of the system we have associated a transverse dipole moment with each molecule which reduces the symmetry of the molecules to C_{2v} . The dispersion interaction has been extensively used in mean field and MC studies [4, 5, 17] to predict the phase behaviour of nematic liquid crystals. The case of symmetric V-shaped molecules considered in the work of Bates [19] can be deduced from the dispersion potential we have used, as has been demonstrated in the work of Romano [22] and Bates and Luckhurst [16]. Although we have used the isotropically averaged out (over the intermolecular vector) form of the dispersion potential (which is short range in nature), the dipolar interactions have been considered in the full form and keeping in mind the long range nature of this interaction we have used the reaction field (RF) method [23, 24] in our calculation to improve the reliability of the results. Although the RF method is less rigorous than the Ewald summation (ES) method, it allows much computational advantages than the latter and the difference of the averages of thermodynamic quantities obtained by the RF and ES techniques are within the statistical uncertainty of the simulation [25, 26, 27]. We have compared our findings with the results of Bates [19] and Grzybowski and Longa [21] and these seem to be in good qualitative agreement. It may be noted that the dispersion potential we have used is a little more general than that in [19] since the former also includes the case of V-shaped molecules with non-symmetric arms. We have also investigated the details of the phase structures of this model by evaluating structural quantities like first-rank and second-rank correlation functions.

2 The Model

In our study we consider identical biaxial molecules with a transverse dipole, whose centers of mass are associated with a simple-cubic lattice. The interaction energy of two molecules

i and j is given by

$$U_{ij} = U_{ij}^{disp} + U_{ij}^{\mu\mu} \quad (1)$$

where U_{ij}^{disp} is the pair potential obtained from London dispersion model [28, 29] and $U_{ij}^{\mu\mu}$ is the dipole-dipole interaction. The dispersion term decays much faster (as $1/r^6$) than the dipolar term (which varies as $1/r^3$). We therefore, restrict the dispersion interaction to the six nearest neighbours. The orientationally anisotropic dispersion interaction explicitly depends both on the mutual orientation of the two interacting molecules, and on their orientations with respect to the intermolecular unit vector ($\hat{\mathbf{r}}_{ij}$). By isotropically averaging over the intermolecular unit vector, $\hat{\mathbf{r}}_{ij}$ the dispersion potential between two identical neighbouring molecules becomes

$$U_{ij}^{disp} = -\epsilon_{ij} \{R_{00}^2(\Omega_{ij}) + 2\lambda[R_{02}^2(\Omega_{ij}) + R_{20}^2(\Omega_{ij})] + 4\lambda^2 R_{22}^2(\Omega_{ij})\}. \quad (2)$$

Here $\Omega_{ij} = \{\phi_{ij}, \theta_{ij}, \psi_{ij}\}$ denotes the triplet of Euler angles defining the relative orientation of i^{th} and j^{th} molecules; we have used the convention used by Rose [30] in defining the Euler angles. ϵ_{ij} is the strength parameter which is assumed to be a positive constant (ϵ) when the particles i and j are nearest neighbours and zero otherwise. R_{mn}^L are combinations of symmetry-adapted (D_{2h}) Wigner functions

$$R_{00}^2 = \frac{3}{2} \cos^2 \theta - \frac{1}{2} \quad (3)$$

$$R_{02}^2 = \frac{\sqrt{6}}{4} \sin^2 \theta \cos 2\psi \quad (4)$$

$$R_{20}^2 = \frac{\sqrt{6}}{4} \sin^2 \theta \cos 2\phi \quad (5)$$

$$R_{22}^2 = \frac{1}{4} (1 + \cos^2 \theta) \cos 2\phi \cos 2\psi - \frac{1}{2} \cos \theta \sin 2\phi \sin 2\psi. \quad (6)$$

The parameter λ is a measure of the molecular biaxiality and depends on the molecular properties. For the dispersion interactions, λ can be expressed in terms of the eigenvalues (ρ_1, ρ_2, ρ_3) of the polarizability tensor $\boldsymbol{\rho}$ of the biaxial molecule

$$\lambda = \sqrt{\frac{3}{2} \frac{\rho_2 - \rho_1}{2\rho_3 - \rho_2 - \rho_1}}. \quad (7)$$

The condition for the maximum biaxiality is $\rho_3 - \rho_2 = \rho_2 - \rho_1 > 0$ and $\lambda = \lambda_C = 1/\sqrt{6}$ (this self-dual geometry corresponds to the Landau point in the phase diagram). $\lambda <$

λ_C corresponds to the case of prolate molecules whereas $\lambda > \lambda_C$ corresponds to oblate molecules. The V-shaped lattice model used by Bates [19] is equivalent to the present dispersion model and it can be shown [16] that both the models produce identical results when the temperature is rescaled properly by using

$$T^* = \frac{4T_{VSM}^*}{(1 - 3 \cos \gamma)^2} \quad (8)$$

and the molecular biaxiality parameter is given by

$$\lambda = \sqrt{\frac{3}{2}} \frac{1 + \cos \gamma}{1 - 3 \cos \gamma} \quad (9)$$

where γ represents the angle between the two symmetric arms of the V-shaped molecule. T^* and T_{VSM}^* are respectively the dimensionless temperatures used in this model and in the V-shaped symmetric model studied by Bates. In general, the biaxiality parameter λ depends both on the inter-arm angle and the relative mesogenic anisotropy of the arms for the symmetric as well as non-symmetric V-shaped molecules [16].

The fully anisotropic biaxial dispersion model has been studied for both two-dimensional and three-dimensional lattices by mean-field and MC methods [31, 22]. The MC simulations performed on a three-dimensional simple cubic lattice system of biaxial molecules interacting via the fully anisotropic dispersion model in one case and its isotropically averaged form in the other case suggest that both the models produce almost similar results [22]. We, therefore, opted the simpler form of the biaxial dispersion pair potential (Eq. (2)) which has been investigated in previous studies and phase diagrams for a fairly wide range of molecular biaxiality have been generated [5, 17].

The dispersion potential (Eq. (2)) can also be expressed in Cartesian form [17] as

$$U_{ij}^{disp} = -\epsilon \left\{ \left[\frac{3}{2} (\mathbf{w}_i \cdot \mathbf{w}_j)^2 - \frac{1}{2} \right] - \lambda \sqrt{6} [(\mathbf{u}_i \cdot \mathbf{u}_j)^2 - (\mathbf{v}_i \cdot \mathbf{v}_j)^2] + \lambda^2 [(\mathbf{u}_i \cdot \mathbf{u}_j)^2 + (\mathbf{v}_i \cdot \mathbf{v}_j)^2 - (\mathbf{u}_i \cdot \mathbf{v}_j)^2 - (\mathbf{v}_i \cdot \mathbf{u}_j)^2] \right\} \quad (10)$$

where \mathbf{u} , \mathbf{v} and \mathbf{w} are the three mutually orthogonal unit vectors along the molecular symmetry axes with the convention [32] that \mathbf{u} and \mathbf{w} are along the shortest and longest axes respectively (Figure 1). Here the orientation of each biaxial molecule, in terms of the Euler angles, with respect to the laboratory frame $\{\mathbf{e}_x, \mathbf{e}_y, \mathbf{e}_z\}$ is given by,

$$\mathbf{u} = (\cos \theta \cos \phi \cos \psi - \sin \phi \sin \psi) \mathbf{e}_x + (\cos \theta \sin \phi \cos \psi + \cos \phi \sin \psi) \mathbf{e}_y - \sin \theta \cos \psi \mathbf{e}_z,$$

$$\mathbf{v} = -(\cos \theta \cos \phi \sin \psi + \sin \phi \cos \psi)\mathbf{e}_x - (\cos \theta \sin \phi \sin \psi - \cos \phi \cos \psi)\mathbf{e}_y + \sin \theta \sin \psi \mathbf{e}_z,$$

and

$$\mathbf{w} = \sin \theta \cos \phi \mathbf{e}_x + \sin \theta \sin \phi \mathbf{e}_y + \cos \theta \mathbf{e}_z.$$

The dipole-dipole interaction for a pair of point dipoles is given by

$$U_{ij}^{dd} = \frac{\mu^2}{4\pi\epsilon_0\sigma^3r_{ij}^3}[(\mathbf{u}_i \cdot \mathbf{u}_j) - 3(\mathbf{u}_i \cdot \hat{\mathbf{r}}_{ij})(\mathbf{u}_j \cdot \hat{\mathbf{r}}_{ij})]. \quad (11)$$

Here $\hat{\mathbf{r}}_{ij}$ is a unit vector along the inter-molecular vector connecting the centres of mass of molecules i and j of the dimensionless separation r_{ij} , μ is the common value of the transverse dipole moment, σ is the nearest neighbour separation and \mathbf{u}_i is the unit vector along the shortest molecular symmetry axis of the i^{th} molecule. The long-range dipolar potential contributions to the total pair potential have been evaluated using the reaction field (RF) method. In this method each dipole is assumed to interact with all others within a spherical cavity of radius r_c and beyond this cutoff radius the dipoles are considered to act as a dielectric continuum of dielectric constant ϵ_s producing a reaction field within the cavity. Therefore the dipolar pair potential within RF geometry can be written as

$$U_{ij}^{\mu\mu} = U_{ij}^{dd} - \frac{2(\epsilon_s - 1)\mu^2 (\mathbf{u}_i \cdot \mathbf{u}_j)}{2\epsilon_s + 1} \frac{1}{4\pi\epsilon_0\sigma^3r_c^3}, \quad (12)$$

for $r_{ij} < r_c$ and $U_{ij}^{\mu\mu} = 0$ for $r_{ij} > r_c$. The truncation must be done for $r_c < L/2$, L being the lattice dimension used in the simulation. The dielectric constant ϵ_s of the surrounding medium is usually chosen to be one of the two extremes, 1 for vacuum or ∞ for conductor. But a self consistent method [25] for estimating ϵ_s during the simulations is most appropriate in the RF method. We have used a parameter

$$\epsilon^* = \frac{\mu^2}{4\pi\epsilon_0\epsilon\sigma^3} \quad (13)$$

which determines the relative strength of the dipolar interaction to the dispersion interaction. For a given value of ϵ^* the relative contribution of the dipolar energy in the total energy at the lowest temperature can be estimated by evaluating the ratio $2.676\epsilon^*/(4.0 + 2.676\epsilon^*)$ where the numerator is related to the negative of the ground-state energy (per particle) of a simple cubic dipolar lattice system [33] whereas the first term in the denominator is the negative of the lowest value (per particle) of the dispersion energy for the optimal value of the molecular biaxiality $\lambda = 1/\sqrt{6}$. The dimensionless temperature used is defined as $T^* = k_B T/\epsilon$.

3 Computational Aspects

To explore phase diagrams we performed a series of Monte Carlo (MC) simulations using the conventional Metropolis algorithm on a periodically repeated simple cubic lattice model, consisting of $N = 40^3$ particles. Simulations were run in cascade, in order of increasing dimensionless temperature T^* . Equilibration runs were typically of 20 000 sweeps where each sweep consisted of N MC steps (or moves) and were followed by a production run of 20 000 – 30 000 sweeps (longer runs were used close to the transitions).

In our case a Monte Carlo move was attempted by selecting a site at random and then by choosing one of the laboratory axes at random the molecule at that site was rotated about the chosen laboratory axis following the Barker-Watts method [34]. The dipolar energy of the molecules has been computed using the RF method, with cut off $r_c = 8$ (in units of lattice spacing). The effect of the cut off radius on the simulation results have been studied in [35, 36]. In our case further increase in r_c produces almost indistinguishable results but increases the computation time significantly. For example if we choose $r_c = 10$ the averaged quantities like order parameters and internal energy change by less than 0.1% compared to the results obtained for $r_c = 8$. However, the CPU time was 62 hours for the former case and is about 28 hours for $r_c = 8$ for simulation at a given temperature with 20 000 Monte Carlo steps per site on Intel Core *i7* 960 processors clocked at 3.2 GHz. The dielectric constant ϵ_s has been evaluated using a self consistent method [25]. In order to analyze the orientational order we have calculated the order parameters $\langle R_{mn}^2 \rangle$ following the procedure described in [37]. According to this, a \mathbf{Q} tensor is defined for the molecular axes associated with a reference molecule. For an arbitrary unit vector \mathbf{w} , the elements of the \mathbf{Q} tensor are defined as

$$Q_{\alpha\beta}(\mathbf{w}) = \langle (3w_\alpha w_\beta - \delta_{\alpha\beta})/2 \rangle \quad (14)$$

where the average is taken over configurations and the subscripts α and β label Cartesian components of \mathbf{w} w.r.t the laboratory frame. The three \mathbf{Q} tensors associated with three molecular symmetry axes are diagonalized (once after each MC sweep) and the eigenvalues and the eigenvectors obtained are then recombined to give the order parameters $\langle R_{mn}^2 \rangle$ w.r.t the director frame [37].

Of the four second rank order parameters only $\langle R_{00}^2 \rangle$ and $\langle R_{22}^2 \rangle$ are of importance in

practice. $\langle R_{00}^2 \rangle$ is the usual uniaxial order parameter $\langle P_2 \rangle$ which measures the alignment of the longest molecular symmetry axis with the primary director (\mathbf{n}) and $\langle R_{22}^2 \rangle$ is the measure of the alignment of the transverse molecular symmetry axes about the secondary directors (\mathbf{l} , \mathbf{m}). $\langle R_{00}^2 \rangle$ is zero in an I phase and it is non-zero in the N_U phase as well as in the N_B phase with maximum value 1 in the perfectly ordered state. On the other hand $\langle R_{22}^2 \rangle$ is zero in the I phase and also in the N_U phase and is non-zero only in the N_B phase and increases towards its maximum value of 0.5 in perfectly ordered biaxial phase.

We have also calculated the reduced specific heat per particle from fluctuations in the energy

$$C_V^* = \frac{\langle E^2 \rangle - \langle E \rangle^2}{Nk_B T^2} \quad (15)$$

where E is the total energy of the system.

Further details on the phase structure of the N_B phase in presence of transverse dipoles can be found by analyzing structural quantities, like the first-rank orientational correlation function defined by

$$g_1(r) = \langle P_1(\mathbf{u}_1 \cdot \mathbf{u}_2) \rangle_r, \quad (16)$$

and the second-rank orientational correlation function,

$$g_2(r) = \langle P_2(\mathbf{u}_1 \cdot \mathbf{u}_2) \rangle_r. \quad (17)$$

The first, which is essentially just the average cosine of the angle between the transverse symmetry axes of molecule 1 and molecule 2 separated by a distance r , is used to determine the anti-ferroelectric structure of the biaxial phase, while $g_2(r)$ is useful in assessing the ordering of the transverse molecular symmetry axes irrespective of their parallel or antiparallel arrangements.

4 Results and discussion

We present phase diagrams for five different values of the relative strength factor $\epsilon^* = 0, 0.4, 0.8, 1.2,$ and 1.6 . The different phases are identified from the non-vanishing values of the relevant order parameters while the transition temperatures are obtained from the positions of the peaks in the temperature dependence of the specific heat curves (C_V^*) as well as from the order parameter curves and these were found to match with each other

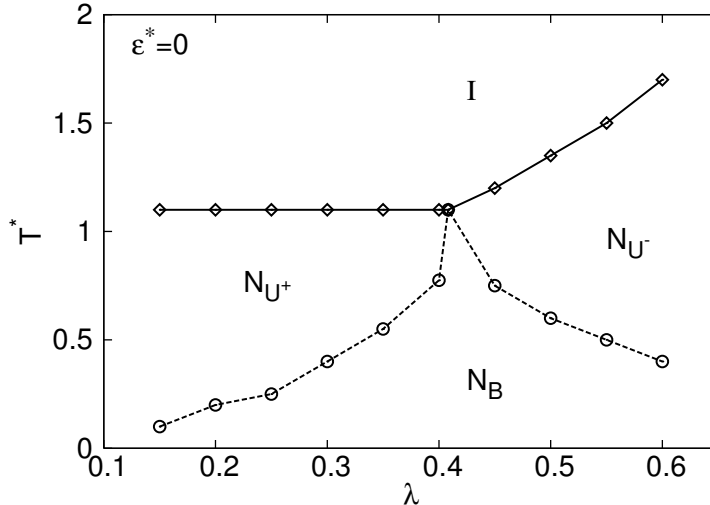


Figure 2: The phase diagram as a function of dimensionless temperature T^* and molecular biaxiality λ (ranging from 0.15 to 0.6 in step of 0.05 along with the self-dual value of 0.40825) for a system of biaxial molecules interacting via second rank anisotropic dispersion potential only. The solid line represents the first-order transitions, while the dashed line represents the second-order transitions.

within the errors present in the simulation. In the neighbourhood of a transition we have taken numerical data at temperature intervals of 0.025 and elsewhere the intervals were greater. To make a conclusion about the order of the phase transitions we have used the order parameter curves – for continuous vanishing of an order parameter the transition was taken as second order whereas a jump to zero or near zero value (which is a finite size effect) from a finite value was considered to be first order transition. These observations were in general supported by our results on specific heat plots. At a second order phase transition the peak heights are relatively smaller than those in a first order transition where the peaks are narrow and sharp. It may be noted that this method of identifying the phase transition temperatures and the order of the transition is only qualitatively correct. To ascertain these accurately one needs to perform more extensive MC simulation using, for instance, the finite size scaling methods which involve collecting data on systems of different size. We did not go into this exercise and therefore expect our results only to be qualitatively correct.

In Figure 2 we have shown the phase diagram for $\epsilon^* = 0$ which means that only the isotropically averaged dispersion interaction (confined to nearest neighbours) given by Eq.

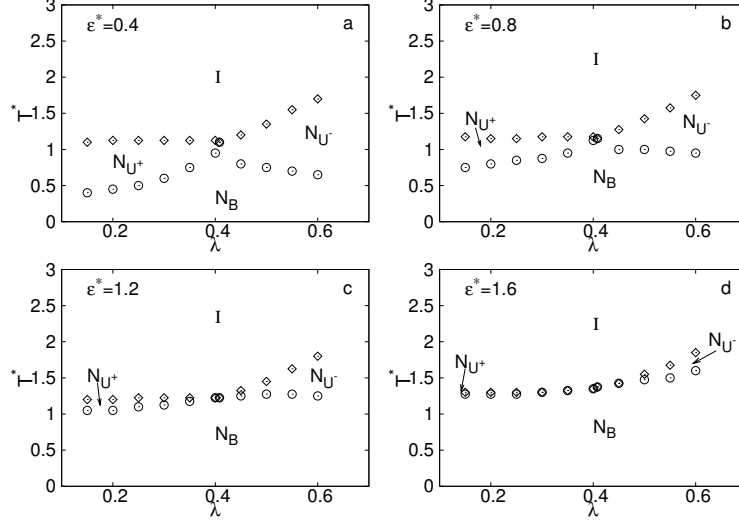


Figure 3: The phase diagrams of biaxial molecules interacting via the resultant potential with four different dipolar strengths $\epsilon^* = 0.4, 0.8, 1.2, 1.6$.

(2) has been considered. The result is same as obtained by Biscarini et al [5] and shows the I , N_{U+} , N_{U-} and the N_B phases. The biaxiality factor λ has been varied from 0.15 to 0.6. The $N_B \leftrightarrow N_U$ transition is found to be second-order while $N_U \leftrightarrow I$ transition is first-order in nature and these are well known from previous studies [2, 3, 5, 11]. At the Landau point (i.e. for $\lambda = 1/\sqrt{6} \approx 0.40825$) a direct $N_B \leftrightarrow I$ transition takes place and this is second-order in nature. In Figure 3 we have shown the phase diagrams when the long range interactions among the transverse dipoles have been considered in addition to the dispersion potential. The diagrams have been plotted for four values of the relative dipolar strength $\epsilon^* = 0.4, 0.8, 1.2$, and 1.6 . When the strength of the dipolar interaction is weak ($\epsilon^* = 0.4$ and 0.8) the higher transition temperature $T_{N_U I}^*$ remains almost unaltered but the presence of (transverse) dipolar interaction stabilizes the N_B phase by raising the temperature $T_{N_B N_U}^*$ to higher value. By increasing the relative dipolar strength, ϵ^* to 1.2 an indication of the formation of Landau line is observed and for strong dipolar interaction ($\epsilon^* = 1.6$) the $N_B \leftrightarrow I$ transition occurs for a range of values of the biaxiality factor λ (from 0.3 to 0.45) instead of a single value. Thus the Landau point (for $\epsilon^* = 0$) turns into a Landau line in presence of strong transverse dipole moments (Figure 3d). Besides performing detail study for ϵ^* upto 1.6 we have performed a search for the extension of the Landau line for $\epsilon^* = 2.0, 2.4$ and 2.8 , where simulations were performed only to locate the two ends of the Landau lines.

We have observed, that the formation of Landau line starts at $\epsilon^* = 1.2$ and the width of the Landau line i.e. range of the values of λ showing the direct $N_B \leftrightarrow I$ transition, first increases and becomes maximum extending from $\lambda = 0.15$ to 0.5 for $\epsilon^* = 2.0$ at which the dipolar interaction is approximately 57% of the total energy at very low temperature. For further increase in the dipolar strength the width of the direct $N_B \leftrightarrow I$ transition becomes shorter and gets shifted towards higher values of λ . For example when $\epsilon^* = 2.4$, the Landau region covers the range of biaxiality parameter from $\lambda = 0.35$ to 0.55 and for $\epsilon^* = 2.8$ it extends from $\lambda = 0.55$ to 0.7 .

We make a qualitative comparison of our findings with those of Grzybowski and Longa [21]. These authors used GB interaction between two-segment and three-segment molecules and also considered the effect of attaching a transverse dipole to each molecule. For two-segment molecules they do not find any Landau line resulting from the presence of the dipoles. This is in disagreement with our observation and with those of Bates [19]. Moreover, we observe that after the formation of Landau line, with increase in the strength of the dipoles the extension of the Landau line first increases, reaches a maximum and then shrinks, always moving towards higher values of λ . Grzybowski and Longa [21] for three-segment GB molecules find the same features in the extension of the Landau line. But initially this happens for lower values of the apex angle γ (i.e. higher λ) and beyond a certain value of the dipole strength the Landau line, which is of smaller extension, occurs at higher values of γ . Moreover, we observe that the most favourable situation (in terms of the width of the Landau line) for the occurrence of the N_B phase occurs for $\epsilon^* = 2.0$. If one considers the lattice spacings (σ) to be of the order of 5\AA and uses the relation in Eq. (13) [38], then for a transition temperature of 473 K (which is close to that of the V-shaped molecule used in [12]), the estimated value of the dipole moment turns out to be 3.3 D which is close to the value of μ obtained in [21]. Here we have used the reduced transition temperature to be 1.5 to estimate ϵ .

We now make a comparison of our results with those of Bates [19]. Bates observed that as the dipolar strength is increased, there is an increase in the $N_B \leftrightarrow N_U$ transition temperature. For $\epsilon^* = 0.5$ the temperature at which the N_B phase is observed is essentially independent of γ (or, λ) and this is just below the temperature at which the Landau point is observed for $\epsilon^* = 0$. This feature is similar to our phase diagram shown in Figure 3c for

$\epsilon^* = 1.2$. We are also inclined to state that for this value of the dipolar strength we find that the Landau line just begins to appear. Moreover, Bates' work shows that for $\epsilon^* = 1.0$ there is a Landau line extending from $\gamma = 107^\circ$ to 122° (the corresponding biaxiality parameter λ being from 0.46 and 0.22) across which there is a first order $N_B \leftrightarrow I$ transition. This may be compared with our observation for $\epsilon^* = 1.6$ where we find a Landau line extending from $\lambda = 0.30$ to 0.45 across which there is a first order $N_B \leftrightarrow I$ transition. We however point out that a direct comparison of our results with those of Bates is not meaningful because of different features appearing in the phase diagrams for different values of the dipolar strengths. This is not surprising since the treatment of the long range dipolar interactions using the RF method rather than truncating it at the nearest neighbours is likely to make this difference. To state this more clearly, the qualitative features observed by Bates now appear at an enhanced value of ϵ^* . Also, while comparing the two sets of results, we need to rescale the temperatures using Eq. (8).

In Figures 4 and 5 we show the plots of C_V^* for $\lambda = 0.3$, and $\lambda = 0.40825$ respectively for the case of pure dispersion interaction ($\epsilon^* = 0$) and for two other cases with relative dipolar strengths $\epsilon^* = 0.8$ and 1.6. In Figure 4a, which is for $\epsilon^* = 0$ and therefore corresponds to the phase point at $\lambda = 0.3$ in Figure 2, we find that C_V^* exhibits two peaks. The smaller peak at low temperature ($T_{N_B N_U}^* = 0.40$) is for a $N_B \leftrightarrow N_U$ transition and the sharper peak at higher temperature ($T_{N_U I}^* = 1.10$) is for the $N_U \leftrightarrow I$ transition. In Figure 4b ($\epsilon^* = 0.8$) the two peaks of C_V^* become closer due to the presence of dipolar interaction ($T_{N_B N_U}^* = 0.85$, $T_{N_U I}^* = 1.175$). In Figure 4c ($\epsilon^* = 1.6$) a single sharp peak in C_V^* is obtained which has a greater height and also occurs at a higher temperature ($T_{N_B I}^* = 1.30$) indicating the formation of the Landau line. In Figure 5a we find a single broad hump in the specific heat plot for $\lambda = 0.40825$ and $\epsilon^* = 0$ which is similar to the earlier findings [5]. Figures 5b and 5c exhibit the influence of the dipolar strengths on C_V^* vs T^* curves at the Landau point. We see that with the increase in dipolar strength the peak height increases and the transition temperature $T_{N_B I}^*$ shifts towards higher value.

The temperature dependence of the second rank order parameters $\langle R_{00}^2 \rangle$ and $\langle R_{22}^2 \rangle$ for $\epsilon^* = 0, 0.8$ and 1.6 and for two different values of the biaxiality factor $\lambda = 0.3$ and 0.40825 are shown in Figure 6 and 7 respectively. In Figure 6a, which is for $\epsilon^* = 0$ we find that the uniaxial and biaxial order parameters $\langle R_{00}^2 \rangle$ and $\langle R_{22}^2 \rangle$ represent order-disorder transitions

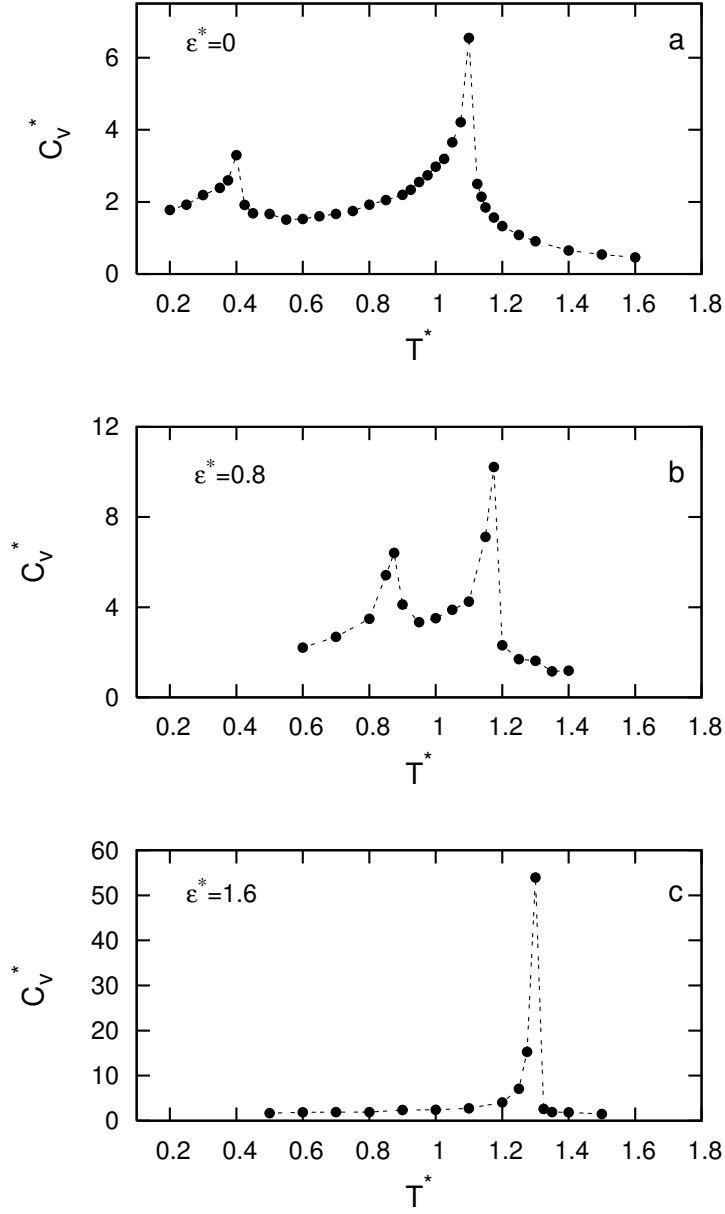


Figure 4: Specific heat per particle vs dimensionless temperature T^* for the molecular biaxiality $\lambda = 0.3$ and for three different dipolar strengths $\epsilon^* = 0, 0.8, 1.6$.

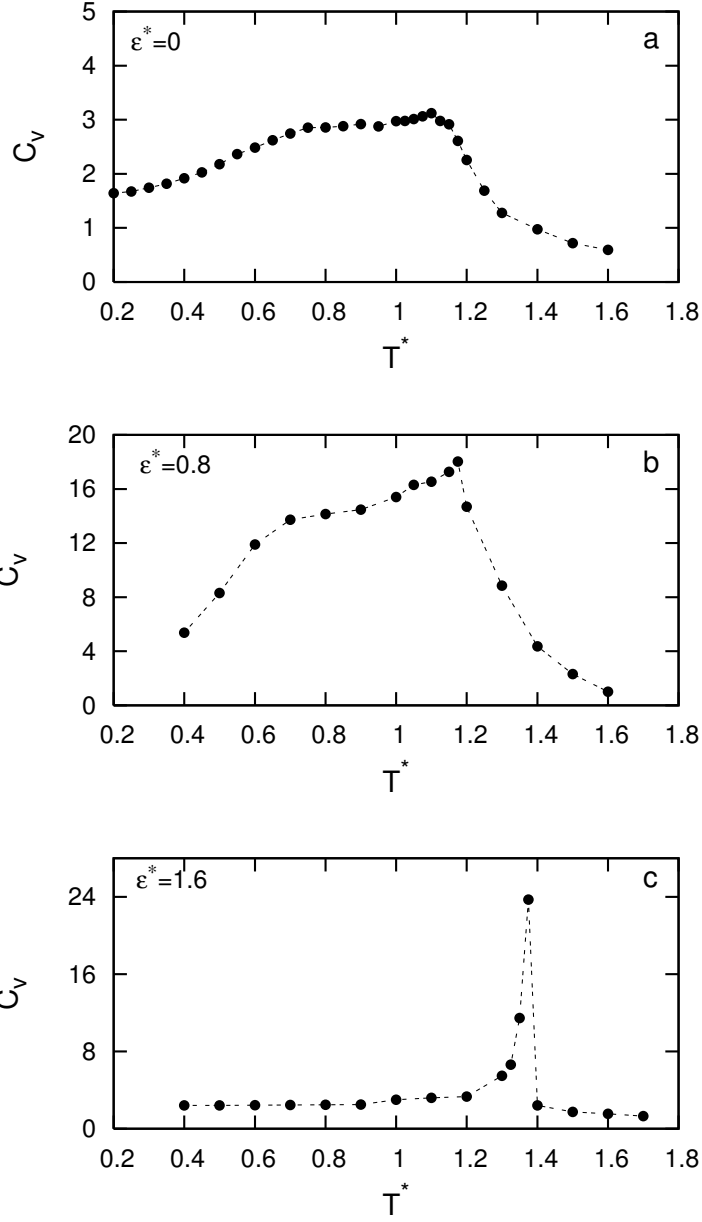


Figure 5: Specific heat per particle vs dimensionless temperature T^* for the molecular biaxiality parameter $\lambda = 0.40825$ and for three different dipolar strengths $\epsilon^* = 0, 0.8, 1.6$.

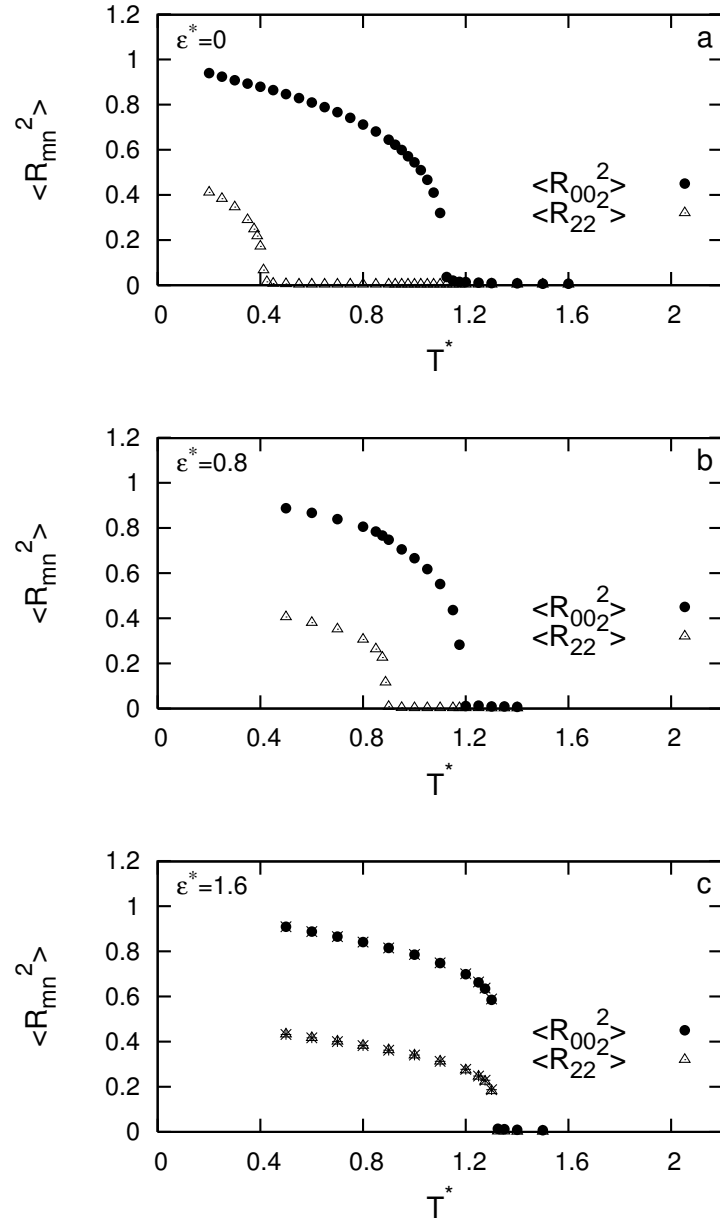


Figure 6: The average second rank (uniaxial and biaxial) nematic order parameters R_{mn}^2 vs dimensionless temperature T^* for the molecular biaxiality parameter $\lambda = 0.3$ and for three different dipolar strengths $\epsilon^* = 0, 0.8, 1.6$.

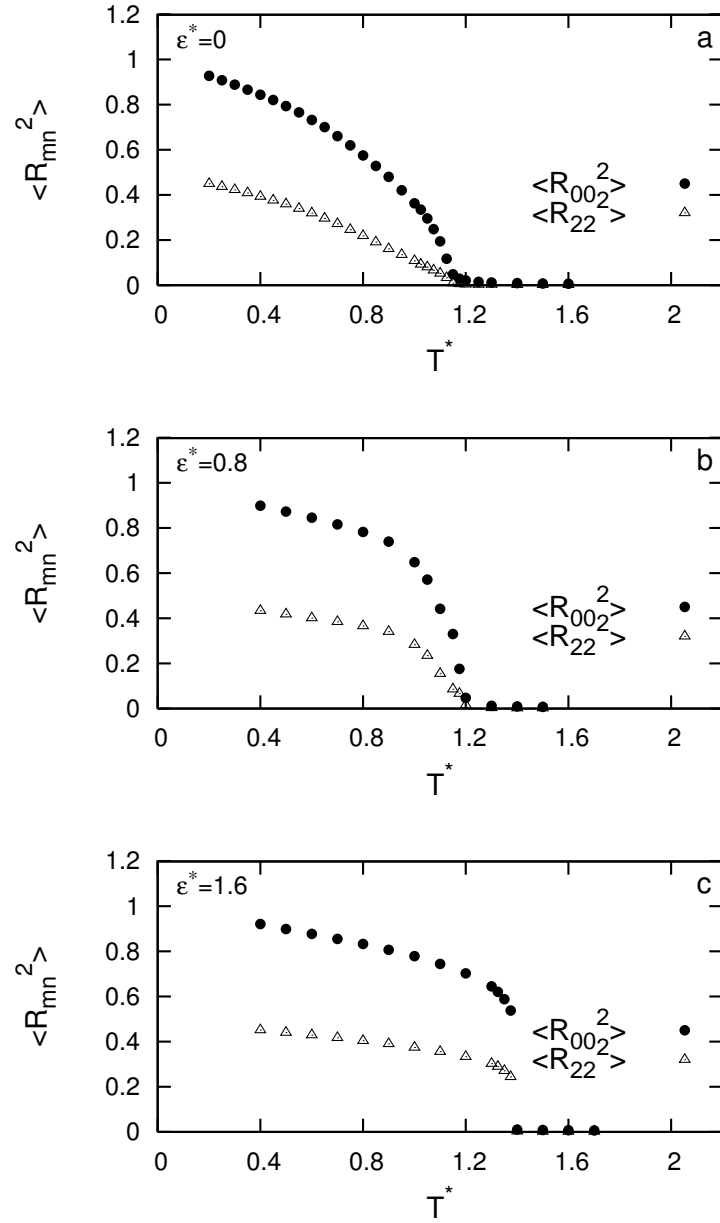


Figure 7: The average second rank (uniaxial and biaxial) nematic order parameters R_{mn}^2 vs dimensionless temperature T^* for the molecular biaxiality parameter $\lambda = 0.40825$ and for three different dipolar strengths $\epsilon^* = 0, 0.8, 1.6$.

at two well separated temperatures. The biaxial order parameter $\langle R_{22}^2 \rangle$ decays continuously almost from its maximum value of 0.5 to 0 at the $N_B \leftrightarrow N_U$ transition ($T_{N_B N_U}^* = 0.40$) whereas the uniaxial order parameter $\langle R_{00}^2 \rangle$ decreases with the increase in T^* and jumps to zero at the $N_U \leftrightarrow I$ transition ($T_{N_U I}^* = 1.10$) which is an well known weakly first order transition. In Figure 6b ($\epsilon^* = 0.8$) both the $N_B \leftrightarrow N_U$ and $N_U \leftrightarrow I$ transitions get shifted towards higher T^* and at the same time become closer due to the presence of dipolar interaction ($T_{N_B N_U}^* = 0.85$, $T_{N_U I}^* = 1.175$). In Figure 6c ($\epsilon^* = 1.6$) both the transitions transform into a single direct $N_B \leftrightarrow I$ transition at a higher temperature ($T_{N_B I}^* = 1.30$). The behaviour of $\langle R_{00}^2 \rangle$ and $\langle R_{22}^2 \rangle$ with T^* in Figure 7a for $\epsilon^* = 0$ and $\lambda = 0.40825$ qualitatively reveal the continuous nature of the direct $N_B \leftrightarrow I$ transition ($T_{N_B I}^* = 1.10$). The increase of strength of the dipolar interaction to $\epsilon^* = 1.6$ (Figure 7c) introduces a distinct change in character of the direct transition. In these figures sharp jumps in the values of $\langle R_{00}^2 \rangle$ and $\langle R_{22}^2 \rangle$ from a considerable finite value to nearly zero values are observed as T^* is gradually increased ($T_{N_B I}^* = 1.375$).

We have also calculated the first rank polar order parameter $\langle P_1^u \rangle = \langle \mathbf{u}_i \cdot \mathbf{l} \rangle$ which is a measure of the degree of alignment of the transverse molecular symmetry axis \mathbf{u} relative to the \mathbf{l} direction of the director frame. We observe that this remains almost zero (within statistical error) over the entire temperature range for different values of the molecular biaxiality parameters and for all dipole strengths. Therefore, in any stable phase the system does not develop any spontaneous polarization. The ground state of the simple cubic system in presence of the dipolar interaction (U_{dd}) alone is anti-ferroelectric and hence does not produce any net overall polarization. This is in agreement with the prediction made by Bates [19] for a system of real dipolar bent core molecules although with the Heisenberg form of dipolar interaction used by Bates is likely to yield a polar phase at low temperature for strong dipole moments. It may be pointed out that the dipolar interaction used in reference [19] is obtained by averaging out the anisotropic dipolar interaction over all orientations of the intermolecular vector for the nearest neighbours in a simple cubic lattice whereas our finding of the absence of a polar phase is obtained with the full form of the dipole-dipole interaction including its long range character.

The orientational correlations between the transverse molecular symmetry axes are represented by plotting the first-rank and the second-rank orientational correlation functions

$g_1(r)$ and $g_2(r)$, defined in Section 3, as a function of molecular separation r in Figure 8 for the molecular biaxiality $\lambda = 0.3$. In case of pure dispersion interaction ($\epsilon^* = 0$) the N_B phase at lower temperature ($T^* = 0.3$) has a long-range behaviour of $g_2(r)$ (Figure 8a). The long-range limit of $g_2(r)$ (0.537) agrees with the square of the corresponding order parameter (which is 0.728), according to the relation

$$\lim_{r \rightarrow \infty} g_2(r) = \left(\left\langle \frac{3}{2} (\mathbf{u}_i \cdot \mathbf{l})^2 - \frac{1}{2} \right\rangle \right)^2. \quad (18)$$

We see that $g_1(r)$ is zero for all values of r which shows, as can be anticipated, that the transverse molecular symmetry axis \mathbf{u} has head tail symmetry in absence of transverse dipoles.

At higher temperature ($T^* = 0.8$), the long range order of the anti-ferroelectric structure in the N_B phase, induced by dipolar interaction ($\epsilon^* = 0.8$), is observed from the pronounced oscillations of $g_1(r)$ as shown in Figure 8b. The positive value of $g_1(r)$ indicates a parallel arrangement of the pair of dipoles whereas its negative value shows their antiparallel arrangement. The oscillations of $g_1(r)$ is non-symmetric about the zero axis because of the typical columnar anti-ferroelectric structure of the simple cubic dipolar system. In a perfectly ordered state out of the six nearest-neighbours ($r = 1$) of a dipole two dipoles are parallel while four are antiparallel and therefore $g_1(r)$ is $-1/3$. For the case of next nearest-neighbours ($r = 2$) all six dipoles are parallel and therefore $g_1(r)$ is 1. For this case the long range behaviour of $g_2(r)$ (Figure 8b) is observed and its long range limit (0.427) is also found to agree with the square of the corresponding order-parameter (0.642) according to Eq. (18).

In Figure 8c we see that in the N_{U+} phase ($T^* = 1.0$) in spite of the presence of dipolar interaction ($\epsilon^* = 0.8$) no anti-ferroelectric structure results. This is observed from the absence of long-range behaviour of $g_1(r)$. $g_1(r)$ remains zero for all values of r except within the first two neighbours where a small oscillation occurs. Also from the variation of $g_2(r)$ it is found that no long-range correlation of the transverse molecular axis is present which confirms the absence of biaxial order. Due to finite size effect a non-zero value (~ 0.1) of $g_2(r)$ is observed at large r which does not correspond to any true long range order for this case.

Since in our study the dipolar part of the total pair potential depends on the orientation of the intermolecular vector, we have found, as expected from a previous study [39], that

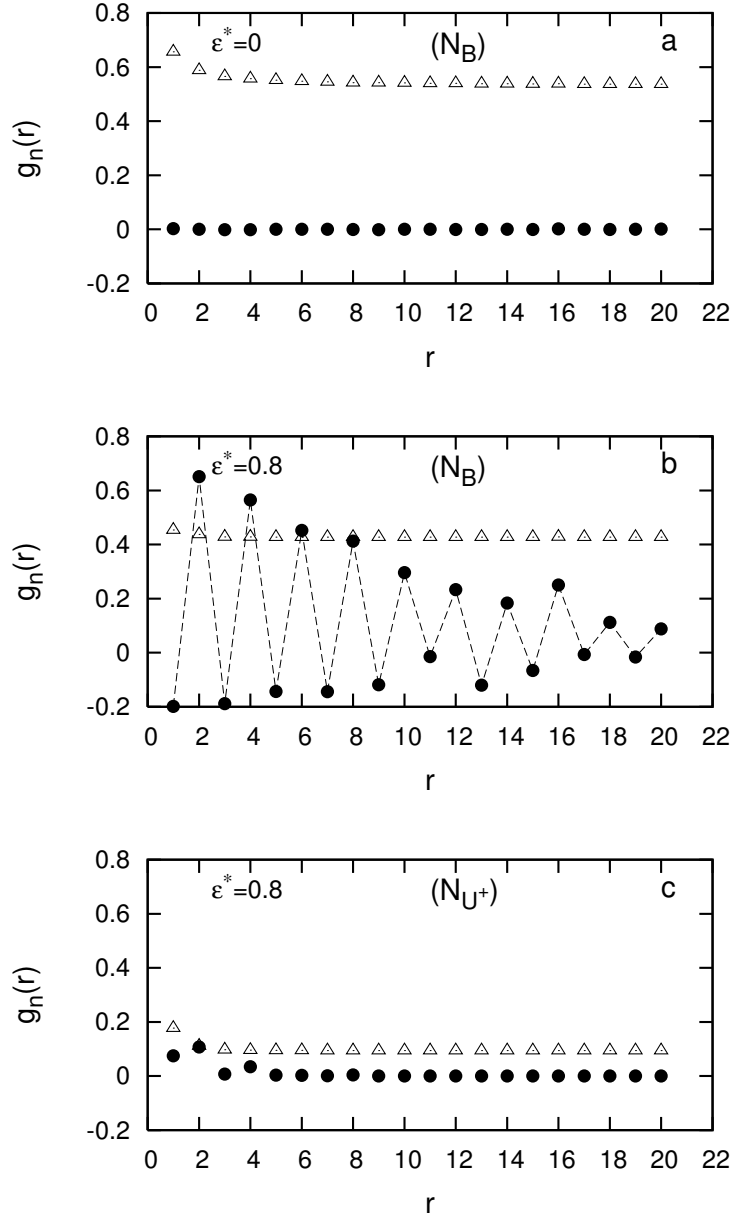


Figure 8: The first-rank and second-rank orientational correlation functions $g_1(r)$ (circles) and $g_2(r)$ (triangles) for the system of biaxial molecules having biaxiality $\lambda = 0.3$ with and without transverse dipoles at the temperatures (a) $T^* = 0.3$ (N_B), (b) $T^* = 0.8$ (N_B) and (c) $T^* = 1.0$ (N_{U+}). The dashed lines are used (in (b)) as a guide for the eye.

the directors are pinned along the lattice axes. The interaction energy of a pair of dipoles depends on the angle between the dipoles and the angles made by the dipoles with the vector joining them. The lowest energy for an interacting pair of dipoles occurs when they are collinear and directed along the vector joining them. The next minimum occurs when they are antiparallel to each other but perpendicular to the inter-dipolar vector. Therefore, for a simple cubic lattice system the ground state is a columnar anti-ferroelectric where the dipoles of a given row are parallel with one of the lattice axes and nearest-neighbour columns are antiparallel. Hence, due to the presence of anisotropy of dipolar interaction in orientation space the director frame coincides with the laboratory frame within a permutation of axes, or in other words, the principal and the secondary directors are pinned along the lattice axes. In order to verify the above fact we have evaluated the averaged quantities $\langle R_{00}^2 \rangle_{lab}$ and $\langle R_{22}^2 \rangle_{lab}$ which represent the uniaxial and biaxial order parameters with respect to the laboratory frame. The above quantities are calculated simply by taking the averages of R_{00}^2 and R_{22}^2 over the total number particles (i.e. the sample averages) for a given configuration and then by taking averages of these sample averages over large number of equilibrium configurations. The order parameters evaluated in the laboratory frame and their counterparts evaluated in the director frame differ by less than 2%. We have determined $\langle R_{mn}^2 \rangle_{lab}$ for $\lambda = 0.3$ and 0.40825 and dipolar strength $\epsilon^* = 1.6$ for different values of the temperature in ordered state. We have noticed that the directors remain pinned for all the temperatures and even close to the $N_B \leftrightarrow I$ transition they remain firmly pinned.

5 Conclusion

The phase diagrams of biaxial molecules possessing D_{2h} symmetry and with transverse dipoles, along their shortest dimensions, have been studied using Monte Carlo simulation. As already elaborated our results are in good qualitative agreement with those in references [19] and [21]. We find that the phase diagram changes significantly due to the influence of strong (transverse) dipolar interaction. The most significant effect of the presence of transverse dipoles is the splitting of the Landau point into a Landau line. Therefore, a range of geometrical structures of biaxial molecules are able to satisfy the most optimum condition of molecular biaxiality. We find that there is an optimal relative dipolar strength

for $\mu \sim 3.3D$ for which the width of the Landau line becomes maximum and for this optimal value the dipolar interactions have almost an equal contribution of energy with that from the dispersion interactions at low temperature. With further increase in dipolar strength the line begins to shorten and get shifted towards higher molecular biaxiality parameters. As the strength of the dipole is increased, the direct $N_B \leftrightarrow I$ transition temperature increases thus leading to an increase in the stability of the thermotropic N_B phase. The continuous nature of the direct $N_B \leftrightarrow I$ transition at the Landau point for the apolar biaxial system also appears to change because of the dipolar interaction. The sharp rise in the height of the specific heat peak and the sudden jumps in the order parameters at the Landau point due to strong dipolar interactions tend to indicate qualitatively that the nature of the transition becomes first order. A finite size scaling analysis is necessary to confirm this change in character of the phase transition. But considering the long-range nature of the dipolar interaction in simulations it becomes a very time consuming task and is therefore left out for future study. The structural properties in the uniaxial and biaxial phases are investigated by evaluating first rank and second rank orientational correlation functions. The dipole induced long range order of the anti-ferroelectric structure in the N_B phase is observed. The lattice model that we have used is very simple in comparison to real thermotropic liquid crystalline systems because real mesogenic molecules have flexibility [40] and also possess both orientational and translational degrees of freedom.

Finally we make a comment on the use of an anisotropic interaction (here the dipolar one) in a lattice model without taking an average over the orientations of the intermolecular vector. This is likely to result in orientationally ordered phases where the director becomes pinned and the structure of the phases depend on the lattice symmetry. Our observation of the appearance of the dipole induced long-range anti-ferroelectric order may have resulted from this. But we are not inclined to think that the biaxial nematic order we have observed in our work resulted from the use of a lattice model and the manner we have treated the dipolar interaction since the phases were identified by the relevant order parameters. A more elaborate study involving translational degrees of freedom of biaxial molecules with transverse dipole moment may perhaps be helpful.

6 Acknowledgment

One of the authors (NG) acknowledges the award of a teacher fellowship under Faculty Development Programme of the UGC, India.

References

- [1] Freiser, M. J. *Phys. Rev. Lett.* **1970**, *24*, 1041.
- [2] Alben R. *Phys. Rev. Lett.* **1973**, *30*, 778.
- [3] Straley J. P. *Phys. Rev. A* **1974**, *10*, 1881.
- [4] Luckhurst G. R. ; Romano S. *Mol. Phys.* **1980**, *40*, 129.
- [5] Biscarini F. ; Chiccoli C. ; Pasini P. ; Semeria F. ; and Zannoni C. *Phys. Rev. Lett.* **1995**, *75*, 1803.
- [6] Camp P. J. ; Allen M. P. *J. Chem. Phys.* **1997**, *106*, 6681.
- [7] (a) Malthete J. ; Nguyen H. T. ; Levelut A. M. *J. Chem. Soc. Chem. Commun.* **1986**, 1548; (b) Malthete J. ; Nguyen H. T. ; Levelut A. M. *J. Chem. Soc. Chem. Commun.* **1987**, 40; (c) Malthete J. ; Nguyen H. T. ; Levelut A. M. ; Galerne Y. *Compt. Rend. Acad. Sci. Paris* **1986**, *303*, 1073.
- [8] (a) Chandrasekhar S. ; Sadashiva B. K. ; Ratna B. R. ; Raja N. V. **1988**, *Pramana* *30* L491; (b) Chandrasekhar S. ; Ratna B. R. ; Sadashiva B. K. ; Raja N. V. *Mol. Cryst. Liq. Cryst.* **1988**, *165*, 123.
- [9] Longa L. ; Grzybowski P. ; Romano S. ; Virga E. *Phys. Rev. E* **2005**, *71*, 051714.
- [10] Berardi R. ; Muccioli L. ; Orlandi S. ; Ricci M. ; Zannoni C. *J. Phys.: Cond. Matt.* **2008**, *20*, 463101.
- [11] Luckhurst G. R. *Thin Solid Films* **2001**, *393*, 40.
- [12] Madsen L. A. ; Dingemans T. J. ; Nakata M. ; Samulski E. T. *Phys. Rev. Lett.* **2004**, *92*, 145505.

- [13] Acharya B. R. ; Primak A. ; Kumar S. *Phys. Rev. Lett.* **2004**, *92*, 145506.
- [14] Merkel K. ; Kocot A. ; Vij J. K. ; Korlacki R. ; Mehl G. H. ; Meyer T. *Phys. Rev. Lett.* **2004**, *93*, 237801.
- [15] Figueirinhas J. L. ; Cruz C. ; Filip D. ; Feio G. ; Ribeiro A. C. ; Frere Y. ; Meyer T. ; Mehl G. H., *Phys. Rev. Lett.* **2005**, *94*, 107802.
- [16] Bates M. A. ; Luckhurst G. R. *Phys. Rev. E* **2005**, *72*, 051702.
- [17] Chiccoli C. ; Pasini P. ; Semeria F. ; Zannoni C. *Int. J. Mod. Phys. C* **1999**, *10*, 469.
- [18] van den Pol E. ; Petukhov A. V. ; Thies-Weesie D. M. E. ; Byelov D. V. ; Vroege G. J. *Phys. Rev. Lett.* **2009**, *103*, 258301.
- [19] Bates M. A. *Chem. Phys. Lett.* **2007**, *437*, 189.
- [20] Lebwohl P. A. ; Lasher G. *Phys. Rev. A* **1972**, *6*, 426.
- [21] Grzybowski P. ; Longa L. *Phys. Rev. Lett.* **2011**, *107*, 027802; Grzybowski P., arXiv:0907.1044v1 [cond-mat.soft] (2009).
- [22] Romano S. *Physica A* **2004**, *339*, 511.
- [23] Barker J. A. ; Watts R. O. *Mol. Phys.* **1973**, *26*, 789.
- [24] Allen M. P. ; Tildesley A. D. *Computer Simulation of Liquids*; Clarendon Press, Oxford, 1987.
- [25] Gil-Villegas A. ; McGrother S. ; Jackson G. *Mol. Phys.* **1997**, *92*, 723.
- [26] Houssa M. ; Oualid A. ; Rull L. *Mol. Phys.* **1998**, *94*, 439.
- [27] Berardi R. ; Orlandi S. ; Zannoni C. *Int. J. Mod. Phys. C* **1999**, *10*, 477.
- [28] Buckingham A. D. in *Intermolecular Forces* edited by J. O. Hirschfelder (Wiley, London, 1967), Chap. 2 [*Adv. Chem. Phys.* **1967**, *12*, 107].
- [29] Stone A. J. *The Theory of Intermolecular Forces*; Oxford University Press, Oxford, UK, 1997.

- [30] Rose M. E. *Elementary Theory of Angular Momentum* Wiley, New York, 1957.
- [31] Romano S. *Physica A* **2004**, *339*, 491.
- [32] Rosso R. *Liq. Cryst.* **2007**, *34*, 737.
- [33] Romano S. *Nuovo Cim. D* **1987**, *9*, 409.
- [34] Barker J. A. ; Watts R. O *Chem. Phys. Lett.* **1969**, *3*, 144.
- [35] Morrow T. J. ; Smith E. R. *J. Stat. Phys.* **1990**, *61*, 187.
- [36] Steinbach P. J. ; Brooks B. R. *J. Comp. Chem.* **1994**, *15*, 667.
- [37] Allen M. P. *Liq. Cryst.* **1990**, *8*, 499.
- [38] Romano S. *Liq. Cryst.* **1988**, *3*, 323.
- [39] Humphries R. L. ; Luckhurst G. R. ; Romano S. *Mol. Phys.* **1981**, *42*, 1205.
- [40] Bates M. A. *Phys. Rev. E* **2006**, *74*, 061702.